

Doping Dependence of Anisotropic Resistivities in Trilayered Superconductor $\text{Bi}_2\text{Sr}_2\text{Ca}_2\text{Cu}_3\text{O}_{10+\delta}$ (Bi-2223)

Takenori Fujii*

*Department of Applied Physics, Faculty of Science,
Tokyo University of Science, Tokyo 162-8601, Japan*

Ichiro Terasaki

Department of Applied Physics, School of Science and Engineering, Waseda University, Tokyo 169-8555, Japan

Takao Watanabe[†]

NTT Basic Research Laboratories, Kanagawa 243-0198, Japan

Azusa Matsuda

*Department of Applied Physics, Faculty of Science,
Tokyo University of Science, Tokyo 162-8601, Japan
NTT Basic Research Laboratories, Kanagawa 243-0198, Japan*

(Dated: October 29, 2018)

The doping dependence of the thermopower, in-plane resistivity $\rho_{ab}(T)$, out-of-plane resistivity $\rho_c(T)$, and susceptibility has been systematically measured for high-quality single crystal $\text{Bi}_2\text{Sr}_2\text{Ca}_2\text{Cu}_3\text{O}_{10+\delta}$. We found that the transition temperature T_c and pseudogap formation temperature $T_{\rho_c}^*$, below which ρ_c shows a typical upturn, do not change from their optimum values in the "overdoped" region, even though doping actually proceeds. This suggests that, in overdoped region, the bulk T_c is determined by the always underdoped inner plane, which have a large superconducting gap, while the carriers are mostly doped in the outer planes, which have a large phase stiffness.

PACS numbers: 74.25.Fy, 74.62.-c, 74.72.Hs

The Bi-Sr-Ca-Cu-O system consists of many superconducting phases with a number of CuO_2 planes in a unit cell. In the bilayer $\text{Bi}_2\text{Sr}_2\text{CaCu}_2\text{O}_{8+\delta}$ (Bi-2212) system, the CuO_2 planes are homogeneously doped, since these planes are crystallographically equivalent. On the other hand, the trilayered $\text{Bi}_2\text{Sr}_2\text{Ca}_2\text{Cu}_3\text{O}_{10+\delta}$ (Bi-2223) system has two crystallographically inequivalent CuO_2 planes, an inner CuO_2 plane with a square (four) oxygen coordination and two outer CuO_2 planes with a pyramidal (five) oxygen coordination. Then, there is a possibility of inhomogeneous doping among layers. Recently, Kivelson¹ proposed that such a inhomogeneous doping helps to increase T_c and accounts for the higher T_c 's in the multi-layered system. There, a high pairing energy scale is derived from the underdoped planes and a large phase stiffness from the optimally or overdoped ones. The combination of these two may provide a key to achieve the higher T_c in the cuprate system. Therefore, it is very important to study the actual multi-layer system in detail.

In high T_c cuprates, there is a consensus that the sets of CuO_2 planes separated by the blocking layer are only weakly coupled and the interaction between them can be understood as a tunneling process. This is known as the confinement effect from the theoretical point of view². However, it is still unknown whether the confinement works for the CuO_2 planes within the unit cell, that was assumed in the above mentioned Kivelson's theory. The inhomogeneous charge distribution provides a new way of investigating such an effect.

The difference of carrier concentration between the inner and outer planes has been reported in NMR studies of multilayered systems^{3,4,5,6,7,8}. In the case of $(\text{Cu}_{0.6}\text{C}_{0.4})\text{Ba}_2\text{Ca}_3\text{Cu}_4\text{O}_{12+y}$, which consists of two inner planes and two outer planes, it was reported that the magnetic and superconducting properties are distinctly different between the inner and outer planes, and the bulk T_c is triggered by the underdoped inner planes. However, all these experiment were performed by using polycrystalline sample, which is magnetically aligned along the c -axis and there have been few investigations of precise doping dependence of single crystal because high-quality samples of multilayered system have not been available. Here, we have successfully grown high-quality single crystals of the trilayered system Bi-2223⁹, and measured the doping dependence of in-plane resistivity ρ_{ab} , out-of-plane resistivity ρ_c , thermopower S , and normal state susceptibility χ for the first time. Based on the results, we discuss the possibility of charge distribution among the CuO_2 planes and the interaction between the CuO_2 planes within the unit cell.

High-quality single crystals were grown using the traveling solvent floating zone (TSFZ) method⁹. The X-ray diffraction pattern showed only sharp Bi-2223 peaks, confirming the good crystallinity of our samples. The c -axis length was estimated from the fitting method using the Nelson-Riley function. The oxygen content δ was controlled by annealing a sample with varying Ar and O_2 gas flow ratios and/or temperatures. A highly oxygenated

sample was prepared by high O₂ pressure (400 atm) annealing using a hot isostatic pressing (HIP) furnace. The annealing conditions for Bi-2223 samples used in this paper are a: O₂ 5×10⁻³ torr 600°C, b: O₂ 0.01% 600°C, c: O₂ 0.1% 600°C, d: O₂ 1% 600°C, e: O₂ 10% 600°C, f: O₂ 600°C, g: O₂ 500°C, h: O₂ 400°C, i: HIP O₂ 400atm 500°C, (These descriptions are used in all Figures). The superconducting transition temperatures T_c were defined by the onset of the Meissner effect. For normal state susceptibility measurement, we used a large single crystal (≈ 10 mg) and applied high magnetic field (5 T). ρ_{ab} was measured with the standard four-probe method, while ρ_c was measured with four-probe-like method with the voltage contacts attached to the center of the ab plane and the current contacts covering almost all of the remaining surface¹⁰. The thermopower was measured using a steady-state technique, where a temperature gradient of 1 K/cm was generated by a small resistive heater and was monitored by differential thermocouple made of copper-constantan.

Figure 1(a) shows the normalized transition temperature T_c plotted against the relative change of the c -axis length from that of the sample "f". The relation between the T_c and c -axis length of Bi-2212 is also plotted for comparison. (The δ of Bi-2212 is determined by the $P_{O_2} - T$ phase diagram obtained by our previous thermogravimetric measurement¹¹.) The T_c and c -axis length are 89 K, 30.864 Å for optimally-doped Bi-2212 and 108 K, 37.119 Å for Bi-2223 (sample "f") respectively. The c -axis length monotonically decreases with increasing δ both in Bi-2212 and Bi-2223, indicating that oxygen is actually incorporated into crystals. In the case of Bi-2212, reflecting the bell-shaped doping dependence of T_c , which is common behavior in mono- or bilayer cuprates, T_c increases with decreasing c -axis length, reaches its maximum, and then decreases with decreasing c -axis length. On the other hand, T_c of Bi-2223 increases with decreasing c -axis length quite similar to Bi-2212. However, T_c keeps its maximum value¹² when the c -axis length is further decreased.

To confirm the carrier doping in the constant T_c region, we measured the doping dependence of the thermopowers S (Fig. 1(b)). The magnitude of the thermopower monotonically decreases with increasing δ . This result clearly shows that the carrier was doped continuously even in the constant T_c region. The room temperature thermopower is considered to be an universal measure of the doping level¹³. By using this measure, the (average) doping level of sample "f" can be assigned to "optimal" doping. Then, the sample "i" would be assigned to slightly overdoping with carrier concentration about $p=0.185$. Thus it would show the T_c of 102 K, if the carriers were homogeneously doped. We will call, hereafter, the constant T_c region as overdoped region.

The temperature dependence of in-plane resistivity $\rho_{ab}(T)$ with various δ is shown in Fig. 2. The absolute values of ρ_{ab} and the overall slopes $d\rho_{ab}/dT$ monotonically decrease with increasing δ , indicating that the

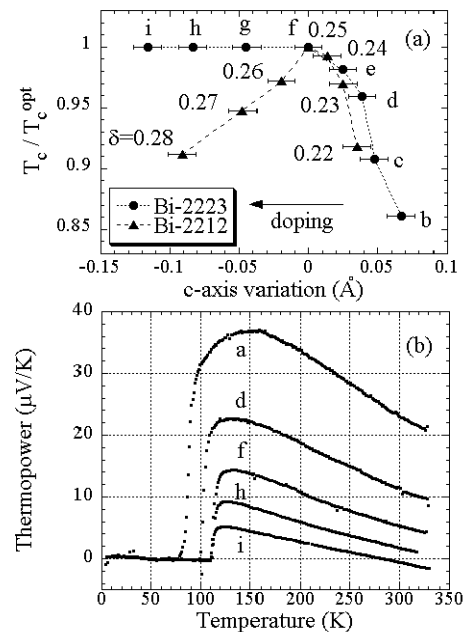


FIG. 1: (a) Normalized transition temperature T_c plotted against the c -axis variation. The T_c and c -axis length of optimum-doping samples are 89 K, 30.864 Å for Bi-2212 and 108 K, 37.119 Å for Bi-2223 respectively. The annealing conditions for Bi-2223 are a: O₂ 5×10⁻³ torr 600°C, b: O₂ 0.01% 600°C, c: O₂ 0.1% 600°C, d: O₂ 1% 600°C, e: O₂ 10% 600°C, f: O₂ 600°C, g: O₂ 500°C, h: O₂ 400°C, i: HIP (O₂ 400atm 500°C), while the δ of Bi-2212 are determined by the $P_{O_2} - T$ phase diagram obtained by our previous thermogravimetric measurement. (b) Thermopower S of Bi₂Sr₂Ca₂Cu₃O_{10+ δ} single crystal annealed in various atmospheres [The labels in Figs. 1, 2, 3, and 4 correspond to each other].

carriers are actually doped with increasing δ . In all doping level, they show negative residual resistivity as indicated by the solid lines in Fig. 2. High- T_c materials with T_c larger than 100 K tend to show negative residual resistivity. The Bi-2223 also seems to belong this class, although we do not know its relevance to T_c . As seen in the inset of Fig. 2, T_c determined by zero resistivity increases from 100 to 110 K with increasing doping level from "b" to "f". However, in the overdoped region, T_c does not change from 110 K. The underdoped samples (denoted by b, d, e, and f) show a downward deviation from high-temperature T -linear behavior below a certain temperature $T_{\rho_{ab}}^*$, similarly to that of Bi-2212¹¹. $T_{\rho_{ab}}^*$ increases with decreasing doping as $T_{\rho_{ab}}^* = 168, 192, 203,$ and 213 K for the samples labeled as f, e, d, and b, respectively as indicated by arrows in Fig. 2. Here, $T_{\rho_{ab}}^*$

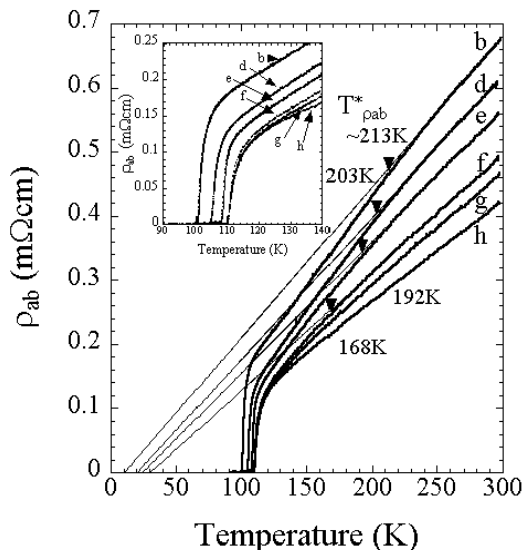


FIG. 2: In-plane resistivity ρ_{ab} of $\text{Bi}_2\text{Sr}_2\text{Ca}_2\text{Cu}_3\text{O}_{10+\delta}$ single crystal annealed in various atmospheres. The solid straight lines, which are linear extrapolations of ρ_{ab} at higher temperatures, are shown as guidelines. The temperatures $T_{\rho_{ab}}^*$ at which the ρ_{ab} deviates from T -linear behavior are shown by arrows. The scale is expanded in the inset for a better view around T_c .

was determined as a temperature at which ρ_{ab} deviates 1% from the high temperature T -linear resistivity using a similar analysis shown in Ref.¹⁴.

Figure 3 shows the c -axis resistivity $\rho_c(T)$ for various δ . Similarly to ρ_{ab} , we can see that T_c is pinned at the maximum value in the overdoped region. The overall magnitude of ρ_c decreases with increasing δ . We have previously shown that the pseudogap formation in the elastic (coherent) tunneling model is an effective explanation for the insulating ρ_c ¹⁵. The decrease in the absolute value of ρ_c with δ would imply an increase in the in-plane density of states (DOS) and semiconductive behavior would be attributed to the decrease of DOS due to the pseudogap formation. The underdoped samples from "a" to "f" show semiconductive ρ_c in all temperature regions measured. As seen in the inset of Fig. 3, in samples "g", "h", and "i", ρ_c decreases linearly with decreasing temperature at higher temperature and show a semiconductive upturn below the characteristic temperature $T_{\rho_c}^*$ (shown by the arrow in the inset of Fig. 3). Here, the straight lines are linear extrapolations of ρ_c at higher temperatures. We estimated $T_{\rho_c}^*$ as the temperature below which ρ_c deviates 1% from the linear straight lines¹⁶. Recent ARPES experiment showed that the pseudogap begins to open from the $(\pi, 0)$ direction (hot spot)^{17,18}. ρ_c should be particularly sensitive to the onset of the pseudogap formation¹⁹, since the hopping probability t_c in the c -axis direction will be dominated by carriers around hot spot on the anisotropic Fermi surface [It is expressed as $t_c \sim (\cos k_x a - \cos k_y a)^2$]²⁰. We can see that the $T_{\rho_c}^*$ remains

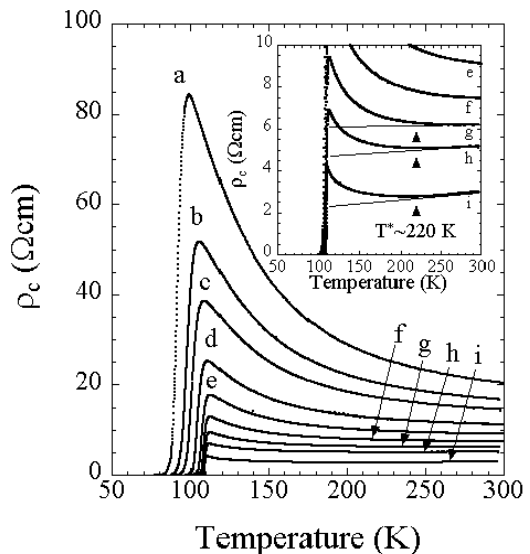


FIG. 3: Out-of-plane resistivity ρ_c of $\text{Bi}_2\text{Sr}_2\text{Ca}_2\text{Cu}_3\text{O}_{10+\delta}$ single crystal annealed in various atmospheres. Overdoped behavior of out-of-plane resistivity is shown in the inset. The solid straight lines in the inset, which are linear extrapolations of ρ_c at higher temperatures, are eye guides for the overdoped sample. Arrows indicate the temperatures $T_{\rho_c}^*$ below which ρ_c shows a characteristic upturn.

unchanged (≈ 220 K) for doping levels higher than "g", while the absolute value of ρ_c continues to decrease.

The magnetic susceptibilities $\chi_{ab}(T)$ for various δ are shown in Fig. 4, where a magnetic field of 5 T was applied parallel to a -axis. The overall magnitude of χ_{ab} monotonically increases with increasing δ . We interpret this in terms of an increase in the DOS near the Fermi level with carrier doping. At all doping levels, the behavior of temperature dependence of χ_{ab} is quite similar to that of Bi-2212¹⁵. The susceptibilities for the underdoped sample (denoted by b, c, and d) monotonically decrease with decreasing temperature, implying a decrease in DOS due to the pseudogap formation. The sample near the optimum-doping level (denoted by f, g, and h) show Pauli paramagnetic behavior at high temperature. And then, the susceptibilities decrease below characteristic temperature T_{χ}^* . T_{χ}^* is estimated as 210, 260, and 315 K for the sample labeled h, g, and f, respectively. Here, T_{χ}^* was determined as the temperature at which χ_{ab} deviates 1% from high-temperature T -linear behavior. Heavily oxygenated (HIPed) sample "i" shows negative temperature dependence ($d\chi/dT \leq 0$), and the dependence is approximately linear. We consider this behavior to be an anomalous DOS effect due to the existence of a van Hove singularity for an overdoped sample^{15,21}.

The anomalous T_c and $T_{\rho_c}^*$ pinning in the overdoped region can be understood by considering inequivalent hole doping between the inner and outer planes. In the overdoped region, the carriers would be mostly doped in the outer planes, and the inner plane would remain at

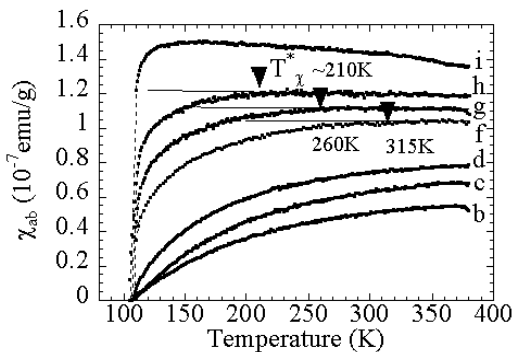


FIG. 4: Magnetic susceptibilities χ_{ab} of $\text{Bi}_2\text{Sr}_2\text{Ca}_2\text{Cu}_3\text{O}_{10+\delta}$ single crystal annealed in various atmospheres. The solid straight lines in the inset, which are linear extrapolations of χ_{ab} at higher temperatures, are eye guides for the overdoped sample. Arrows indicate the temperatures T_{χ}^* at which χ_{ab} start to decrease from its linear high temperature behaviors.

the underdoping level. Here, the coupled system, which Kivelson assumed, seems to be realized. Highest T_c 's would be maintained by the combination of inner plain's large superconducting gap and the outer plain's large superfluid density^{22,23}, which controls the stiffness of the system to phase fluctuations. From the practical point of view, the phase stiffness is very important for sustaining a large superconducting current, as well as T_c . This gives a promising way of improving the characteristics of high T_c materials.

On the other hand, $T_{\rho_c}^*$ pinning in the overdoped region, as well as semiconducting ρ_c behavior, is also determined by the always optimally-doped inner plane, which is known to have a pseudogap. Since the outer planes are overdoped, the transport between outer planes separated by the Bi_2O_2 layer may not show a pseudogap effect. Then the observed pseudogap effect may come from the transport between the outer and inner planes. This indicates that the interaction between the CuO_2 planes within a unit cell is very weak, like that between the CuO_2 planes separated by the blocking layer. Thus, in multilayered system, there already exist an array of weakly coupled planes, which was assumed in the above-mentioned Kivelson's theory.

In Bi-2212, the characteristic temperatures T_{χ}^* and $T_{\rho_c}^*$ coincide for all doping levels and shift to lower temperature with increasing doping level¹⁵. Thus, as mentioned above, semiconductive ρ_c and the decrease in susceptibility are explained by the decrease in the DOS due to the pseudogap formation. However, in Bi-2223, T_{χ}^* does not coincide with $T_{\rho_c}^*$. This is also considered to be result of inequivalent hole doping between the inner and outer

planes. The susceptibility of Bi-2223 is considered to be the sum of the susceptibilities of inner plane and outer planes. Then, the negative temperature dependence in outer planes may conceal the pseudogap effect of the inner plane in the overdoped region, because the overall magnitude and the weight of the outer planes are larger than those of the inner plane.

On the other hand, $T_{\rho_{ab}}^*$ is also considered to be an indication of pseudogap formation^{11,14}, because, in the case of $\text{YBa}_2\text{Cu}_3\text{O}_{6+\delta}$, $T_{\rho_{ab}}^*$ coincides with $T_{\rho_c}^*$ ¹⁶ as well as T_{χ}^* . However, in $\text{Bi}_2\text{Sr}_2\text{CaCu}_2\text{O}_{8+\delta}$ (Bi-2212), we have previously pointed out that $T_{\rho_{ab}}^*$ does not coincide with T_{χ}^* . The same tendency can be seen in the case of Bi-2223. The anomaly seen at $T_{\rho_{ab}}^*$ can be understood if we consider the strongly k -dependent quasiparticle lifetime. The carriers around the hot spot, where the pseudogap first opens up, will not contribute to the in-plane conduction, in contrast to ρ_c .

In summary, we measured a doping dependence of the thermopower, in-plane resistivity, out-of-plane resistivity, and susceptibility of high quality single crystal Bi-2223 for the first time. The room temperature thermopower, as well as the absolute value of resistivity (ρ_{ab} and ρ_c), and c -axis length, continuously decrease with increasing δ , and the overall magnitude of susceptibility increases with increasing δ . All the results indicate that the carrier is properly controlled by our annealing method in the whole doping region. When the doping proceeds from underdoped to optimum-doped, transition temperature T_c increases quite similar to Bi-2212. However, it does not change in the overdoped region. On the other hand, we clearly observed the pseudogap formation in the ρ_{ab} and ρ_c , which is similarly seen in Bi-2212. From the doping dependence of ρ_c , which is very sensitive to the onset of the pseudogap formation, we found that the pseudogap formation temperature T^* does not change from its optimum value in the overdoped region. These results suggest that there is large difference in the carrier concentration between the inner and outer planes and in the overdoped region, the carriers may be mostly doped in the outer planes and the inner plane would remain at the underdoped level. As pointed by Kivelson, the combination of a large superconducting gap Δ in the inner plane and a large superfluid density of the outer planes would help to keep the highest T_c in the overdoped region. On the other hand, $T_{\rho_c}^*$ pinning indicates that the pseudogapped inner plane also determines the c -axis transport property. This suggests that the carriers in the normal state are weakly coupled or confined to individual CuO_2 planes.

* Corresponding author, Present address: Department of Applied Physics, School of Science and Engineering,

Waseda University, Tokyo 169-8555, Japan; Electronic address: fujii@htsc.phys.waseda.ac.jp

- [†] Present address: NTT Photonics Laboratories, Kanagawa 243-0198, JAPAN.
- ¹ S. A. Kivelson, cond-mat 0109151.
 - ² P. W. Anderson, *Physica (Amsterdam)* **C185-189**, 11 (1991).
 - ³ M.-H. P. Carretta, M. Horvatic, C. Berthier, Y. Berthier, P. Segransan, A. Carrington, and D. Colson, *Phys. Rev. Lett.* **76**, 4238 (1996).
 - ⁴ K. Magishi *et al.*, *J. Phys. Soc. Jpn.* **64**, 4561 (1995).
 - ⁵ Y. Tokunaga, K. Ishida, K. Magishi, S. Ohsugi, G. -q. Zheng, Y. Kitaoka, K. Asayama, A. Iyo, K. Tokiwa and H. Ihara, *Physica (Amsterdam)* **B259-261**, 571 (1999).
 - ⁶ Y.V. Piskunov, K. N. Mikhalev, Yu. I. Zhdanov, A. P. Gerashenko, S. V. Verkhovskii, K. A. Okulova, E. Yu. Medvedev, A. Yu. Yakubovskii, L. D. Shustov, P. V. Bellot and A. Trokiner, *Physica (Amsterdam)* **C300**, 225 (1998).
 - ⁷ A. Trokiner, L. Le Noc, J. Schneck, A. M. Pougnet, R. Mellet, J. Primot, H. Savary, and Y. M. Gao, and S. Aubry, *Phys. Rev.* **B44**, 2426 (1991).
 - ⁸ Y. Tokunaga, K. Ishida, Y. Kitaoka, K. Asayama, K. Tokiwa, A. Iyo, and H. Ihara, *Phys. Rev.* **B61**, 9707 (2000).
 - ⁹ T. Fujii, T. Watanabe, and A. Matsuda, *J. Cryst. Growth* **223**, 175 (2001)
 - ¹⁰ T. Watanabe, and A. Matsuda, *Phys. Rev.* **B54**, R6881 (1996).
 - ¹¹ T. Watanabe, T. Fujii, and A. Matsuda, *Phys. Rev. Lett.* **79**, 2113 (1997).
 - ¹² M. Ogino, T. Watanabe, H. Tokiwa, A. Iyo, and H. Ihara, *Physica (Amsterdam)* **C258**, 384 (1996)
 - ¹³ S. D. Obertelli, J. R. Cooper, and J. L. Tallon, *Phys. Rev.* **B46**, 14928 (1992).
 - ¹⁴ T. Ito, K. Takenaka, and S. Uchida, *Phys. Rev. Lett.* **70**, 3995 (1993).
 - ¹⁵ T. Watanabe, T. Fujii, and A. Matsuda, *Phys. Rev. Lett* **84**, 5848 (2000).
 - ¹⁶ K. Takenaka, K. Mizuhashi, H. Takagi, and S. Uchida, *Phys. Rev.* **B50**, 6534 (1994).
 - ¹⁷ D. S. Marshall, D. S. Dessau, A. G. Loeser, C-H. Park, A. Y. Matsuura, J. N. Eckstein, I. Bozovic, P. Fournier, A. Kapitulnik, W. E. Spicer, and Z.-X. Shen, *Phys. Rev. Lett* **76**, 4841 (1996).
 - ¹⁸ M. R. Norman, H. Ding, M. Randeria, J. C. Campuzano, T. Yokoya, T. Takeuchi, T. Takahashi, T. Mochiku, K. Kadowaki, P. Guptasarma, and D. G. Hinks, *Nature (London)* **392**, 157 (1998).
 - ¹⁹ T. Shibauchi, L. Krusin-Elbaum, Ming Li, M. P. Maley, and P. H. Kes, *Phys. Rev. Lett* **86**, 5763 (2001).
 - ²⁰ L. B. Ioffe, and A. J. Millis, *Phys. Rev.* **B58**, 11631 (1998).
 - ²¹ A. Matsuda, S. Sugita, T. Fujii, and T. Watanabe, *J. Phys. Chem. Solids* **62**, 65 (2001)
 - ²² Y. J. Uemura, G. M. Luke, B. J. Sternlieb, J. H. Brewer, J. F. Carolan, W. N. Hardy, R. Kadono, J. R. Kempton, R. F. Kiefl, S. R. Kreitzman, P. Mulhern, T. M. Riseman, D. Ll. Williams, B. X. Yang, S. Uchida, H. Takagi, J. Gopalakrishnan, A. W. Sleight, M. A. Subramanian, C. L. Chien, M. Z. Cieplak, Gang Xiao, V. Y. Lee, B. W. Statt, C. E. Stronach, W. J. Kossler, and X. H. Yu, *Phys. Rev. Lett* **62**, 2317 (1989).
 - ²³ Y. J. Uemura, L. P. Le, G. M. Luke, B. J. Sternlieb, W. D. Wu, J. H. Brewer, T. M. Riseman, C. L. Seaman, M. B. Maple, M. Ishikawa, D. G. Hinks, J. D. Jorgensen, G. Saito, and H. Yamochi, *Phys. Rev. Lett* **66**, 2665 (1991).